INVITED REVIEW PAPER

Strategic use of thermo-chemical processes for plastic waste valorization

Sungyup Jung* and Insoo Ro**,†

*Department of Environmental Engineering, Kyungpook National University, Daegu 41566, Korea
**Department of Chemical and Biomolecular Engineering, Seoul National University of Science and Technology,
Seoul 01811, Korea

Abstract−Plastic is one of the most widely used materials in industries including packaging, building, and construction due to its lightweight, low cost, durability, and versatility. However, the mass production of plastics has exacerbated plastic pollution. Globally, plastic waste is predominantly incinerated, landfilled, or released into the environment; only 5-6% is recycled in the United States. Although conventional management protocols such as incineration and landfilling are evidently effective for plastic waste disposal, they are associated with significant environmental and societal challenges. In addition, most recycled plastic is downcycled, and thus does not provide sufficient incentive to use recycled materials instead of virgin materials. This review discusses thermo-chemical upcycling processes such as (catalytic) pyrolysis and heterogeneous catalysis. Furthermore, we present the recent progress in the thermo-chemical upgrading of single-type plastic waste, heterogeneous plastic mixtures, and post-consumer plastic waste obtained from different locations and, finally, suggest future research directions.

Keywords: Circular Economy, Municipal Solid Waste, Heterogeneous Catalysis, Pyrolysis

INTRODUCTION

Synthetic polymers, namely plastics, have been widely used in a variety of industries as essential materials. Plastic is characterized by features such as high durability, low cost, lightweight, non-biodegradability, convenience of processing, and mass production [1]. Representative applications of plastic materials include packing [2], construction and building materials [3], textile [4], electronic/electrical equipment [5], and agricultural products [6]. With the increasing demand for plastic materials owning to their usefulness, the global consumption of plastic reached 460 million tons in 2019. Currently, plastic consumption has increased by more than 230 times compared with that in 1950 [7]. Substantial amounts of plastic materials are produced owing to their enhanced physicochemical properties, affordability, and the viability of large-scale production; however, the excess generation of plastic waste is an inevitable problem. Particularly, 353 million tons of plastic waste was generated in 2019, corresponding to approximately 80 wt% of the global plastic production [7].

Plastic waste production has become an area of concern because of the rapid increase in the waste generation rate and the low technical readiness level of plastic waste management. In conventional management protocols, plastic waste is primarily landfilled after a short-life span or even after a single use of plastic materials [8,9]. Uncontrolled weathering and natural degradation of plastic waste subsequently releases leachates that contain plastic fragments and invisible microplastics into the environment [6]. For example, microplastics degraded from landfilling sites can contaminate groundwater [10]. Since plastic waste is not biodegradable, its degradation rate is considerably slower than its accumulation rate. Consequently, landfills require additional space, resulting in significant environmental and societal challenges [11]. Incineration is another major disposal protocol for plastic waste. In this process organic plastic materials are rapidly oxidized into gaseous products. The advantage of incineration is that the volume of plastic waste is rapidly reduced, thereby requiring relatively small space for waste treatment [12]. However, owing to the incomplete oxidation of organic waste, incineration releases CO_2 and other hazardous gases into the atmosphere. Considering that plastic materials are synthesized from fossil resources, extensive production of greenhouse gas and toxic chemicals from plastic waste treatment could be a significant contributor to global warming and health problems [13].

Reuse and recycling are promising green approaches to plastic waste material management. However, the overall plastic recycling rate is considerably low. For example, in the United States, only 5 to 6% (approximately 2 million tons out of 40 million tons) of plastic waste was recycled, according to the World Economic Forum [14]. The recycling rate of household plastic waste in Korea is 13.5% (about 0.4 million tons of 3 million tons), and the recovery rate is 37% (about 1.1 million tons for the production of solid refuse fuel) [15]. Moreover, packaging materials such as bottles and containers are typically produced from two types of plastic, namely, polyethylene terephthalate (PET) and high-density polyethylene (HDPE), which have a particularly high recycling rate because they can be simply separated and discharged with less difficulty and contamination [16]. The separately collected high-purity PET and HDPE are converted into granules through washing, crushing, and melting. The granules are subsequently re-used for the formation of end-products composed of PET or HDPE.

Apart from PET and HDPE containers, only small amounts of

---

†To whom correspondence should be addressed.
E-mail: insoo@seoultech.ac.kr

other types of plastic waste are recycled, because the plastic materials are composed of heterogeneous mixtures and plastic additives [17]. Heterogeneous waste mixtures require additional separation and washing before value-added products can be obtained. The pre-treatment processes are labor-intensive and expensive. Thus, high-value products need to be generated via practical plastic waste management and upgrading processes to ensure economic feasibility [18,119,120].

Recently, thermo-chemical upcycling processes such as (catalytic) pyrolysis and heterogeneous catalysis have received considerable attention. The thermo-chemical processes can convert plastic waste into high-value products such as plastic monomers [19], industrial/fuel-range hydrocarbons (HCs) [20], and syngas [21]. Herein, we present the recent progress in thermo-chemical upgrading processes for single-type plastic waste, heterogeneous plastic mixture, and practical plastic waste obtained from different locations. The challenges associated with each thermo-chemical process are discussed. Moreover, we suggest a strategic approach for selecting suitable thermo-chemical processes based on the type of plastic waste. Finally, we discuss the future research direction.
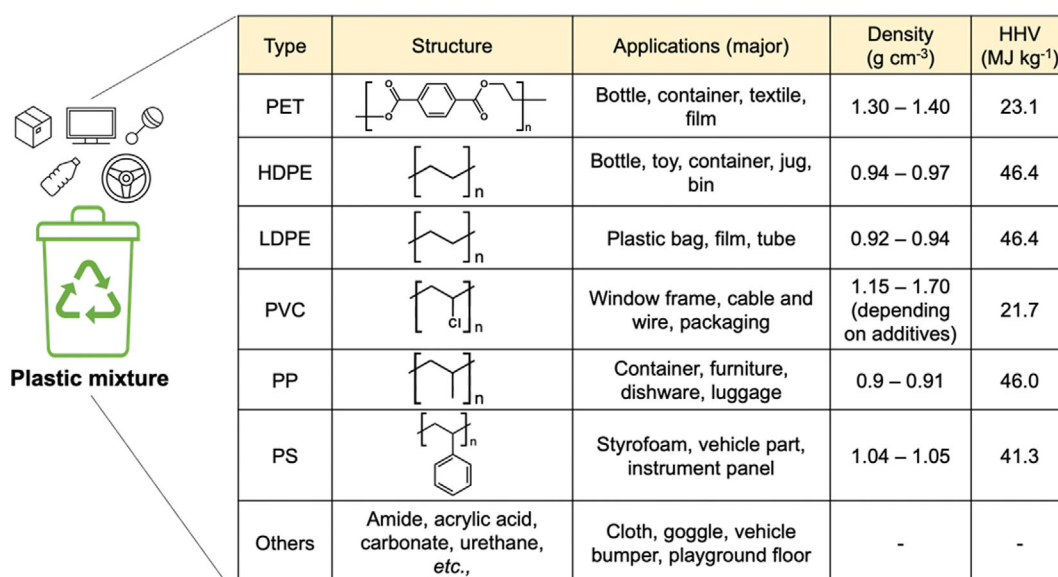
PLASTIC WASTE COMPOSITION AND SEPARATION OF HIGH-PURITY FEEDSTOCK

To reduce municipal solid waste (MSW) generation, plastic waste is separately collected from MSW, which contains other materials such as glass, metal, food waste, and paper. [22]. When the spent plastic waste materials are discarded, they are generally collected in a single plastic waste bin, although the plastic comprises different types of materials (Fig. 1). Post-consumer plastic waste is predominantly composed of heterogeneous mixtures, whereas some products consist of homogeneous plastic (*e.g.*, HDPE containers). In the discharging process, the heterogeneous post-consumer plastic waste is further mixed with other types of plastic. The plastic mixture predominantly contains PET, polyethylene (PE, high and low density), polyvinylchloride (PVC), polypropylene (PP), and polystyrene (PS), as shown in Fig. 1. Other types of plastics, such as polyamide, polyacrylic acid, polycarbonate, and polyurethane, are also included in the plastic waste mixture [16]. Additionally, the plastic waste streams include foreign materials and plastic additives that are used to control the physicochemical properties of plastics [23]. For example, antioxidants, stabilizers, plasticizers, flame retardants, lubricants, slip agents, foaming agents, reinforcements, and colorants are used as additives to control plastic properties [23]. Metal(oxide)s are also used as supporting materials in plastic-based products [24].

High-purity post-consumer plastics are necessary for producing value-added fine chemicals and high-heating value fuels from plastic waste. The collected plastic waste is transferred to centralized recycling facilities to obtain the maximum amount of reusable and recyclable post-consumer plastics [17,22]. The high-purity single plastic stream is obtained through multiple steps, including plastic sorting and washing, which remove additives and contaminants. The plastic waste pretreatment processes prior to thermo-chemical upgrading involve the screening of impurities, plastic/material sorting, size control, and washing [25].

Initially, the collected plastic waste is manually screened by operators who remove visible bulk impurities such as films, glass, aluminum, cardboard, and other large items on the conveyor belt of the plastic waste stream. In the subsequent process, small undesirable materials such as broken glass, stones, and metals are sorted using a rotary drum or/and vibrating sieve [25]. Therefore, pre-screened plastic waste is transferred to different sorting units to obtain high-purity single polymer streams. Plastic/material sorting is the most important step in terms of preparation for a high-purity single plastic stream. Techniques such as gravity, electrostatic, and magnetic separation, flotation, and sensor-based sorting are selectively used depending on the conditions and physicochemical properties of plastics and impurities in the waste stream [25].

Type	Structure	Applications (major)	Density (g cm^{-3})	HHV (MJ kg^{-1})
PET		Bottle, container, textile, film	1.30 – 1.40	23.1
HDPE		Bottle, toy, container, jug, bin	0.94 – 0.97	46.4
LDPE		Plastic bag, film, tube	0.92 – 0.94	46.4
PVC		Window frame, cable and wire, packaging	1.15 – 1.70 (depending on additives)	21.7
PP		Container, furniture, dishware, luggage	0.9 – 0.91	46.0
PS		Styrofoam, vehicle part, instrument panel	1.04 – 1.05	41.3
Others	Amide, acrylic acid, carbonate, urethane, *etc.*,	Cloth, goggle, vehicle bumper, playground floor	-	-

Fig. 1. Major types of plastic collected in plastic mixture waste bins, their applications, and higher heating value (HHV). Density and HHV data were obtained from references [26,27], respectively.
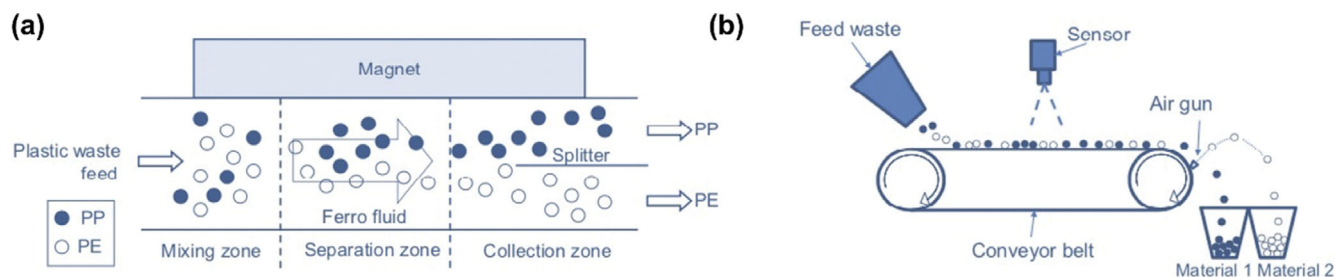
Fig. 2. Schematics of (a) magnetic density separation and (b) sensor-based sorting systems. Reprinted with permission from [25]. Copyright 2019 Elsevier.

In gravity separation units, lighter (e.g., PP, HDPE, and LDPE) and heavier (e.g., PET, PVC, acrylonitrile butadiene styrene (ABS)) plastics can be separated in the waste stream via sink-flotation separation, air classifiers, and cylindrical cyclones [25]. As shown in Fig. 1, a significant density difference between polyolefins (0.9-1.0 g cm^{-3}) and other materials (up to 1.7 g cm^{-3}) facilitates density separation. To further separate each type of plastic, electrostatic separation is employed according to different triboelectric charging sequences of major plastics: (+) ABS - PP - PC - PET - PS - PE - PVC (−) [25,28]. In magnetic density separation, artificial gravity is applied when plastic waste is allowed to pass through the ferrofluid (i.e., liquid stream including iron oxide) [29]. In the presence of the magnetic force, artificial gravity is applied exponentially in the vertical direction, and different types of plastics can be separated through the ferrofluid according to their density (Fig. 2(a)). Magnetic density separation is useful for separating polyolefins such as PP and PE [30]. Sensor-based sorting systems are also considered useful. They comprise three parts: a waste material feeding conveyor belt, a sensor to identify each material, and an automatic system to mechanically separate the materials. An example of mechanical separation via an air gun is shown in Fig. 2(b). Different types of spectroscopy, imaging, and X-ray analyses can be used for identifying each type of plastic [25].

Separated single-type plastic should be further washed units to prepare cleaner feedstocks before thermo-chemical valorization. Sorted plastic is generally washed with clean water in addition to cleaning agents, such as detergents and organic solvents, to remove dirty and odorous contaminants [31]. The cleaning process releases wastewater containing micropollutants, particularly microplastics, into the environment [6,32]. Prior to the thermo-chemical upgrading of the cleaned plastic waste, wet samples may require an additional drying step depending on the upgrading process.

PYROLYSIS OF PLASTIC WASTE

1. Plastic Oil Production through Plastic Pyrolysis

Pyrolysis has been widely employed used for producing fuel oils from plastic waste. Pyrolysis is performed under the anoxic condition to thermally degrade a single type of plastic waste and/or plastic waste mixtures [4,33-35]. When organic plastic materials are thermally degraded, plastic char, oil, and gas are produced owning to the carbon redistribution from solid plastic to three-phase products. Plastic oil production has typically been considered a primary objective of pyrolysis because plastic oils can be used as fuel oils

owing to their high heating value. The higher heating value (HHV) of each plastic type is shown in Fig. 1. Particularly, PE (46.4 MJ kg^{-1}), PP (46.0 MJ kg^{-1}), and PS (41.3 MJ kg^{-1}) have similar HHV to those of gasoline (46.4 MJ kg^{-1}) and diesel (45.6 MJ kg^{-1}), because the plastics and liquid fuels are predominantly composed of carbon and hydrogen [26,27]. Moreover, the fuel efficiency of plastic fuel is comparable to that of diesel fuel [36,37].

However, other major plastics such as PET (23.1 MJ kg^{-1}) and PVC (21.7 MJ kg^{-1}) have relatively lower HHV owing to their high oxygen content and the presence of heteroatoms [38,39]. In addition, PET and PVC remain as solid residues (i.e., plastic char) after thermolysis even at temperatures higher than 900 $^{\circ}$C [40,41]. Despite numerous studies on the relationships between the reaction conditions and products resulting from plastic pyrolysis, previous studies on plastic pyrolysis are categorized into three main themes: (1) production of fuel range HCs from the pyrolysis of polyolefins and their mixtures, (2) production of flammable gases from low heating value plastics and different mixtures, and (3) utilization of the remaining solid residue char.

PE and PP, the most extensively used plastics, have received considerable interest with reference to plastic oil products for which high-purity PE, PP, and their mixtures are used as reactants in the pyrolysis process. Previous review papers comprehensively discussed the pyrolysis of PE and PP [34,42]. As summarized in Table 1, plastic oils are the primary products obtained from pyrolyzing PE, PP, and their mixtures in the temperature range of 420-550 $^{\circ}$C. The major chemical compounds in plastic oils are C$_{5-40}$ aliphatic HCs (C$_{5-40}$), which are similar to those in gasoline, diesel, jet fuel, and fuel oil [43]. PS also has been converted into plastic oil. Because styrene monomer is a repeating unit of PS, thermal degradation of PS during pyrolysis results in the production of a styrene monomer, dimer, and trimer as the main compounds (Table 1). Considering that practical liquid transportation fuels are primarily composed of aliphatic HCs in addition to benzene derivatives, plastic oils derived from polyolefin mixtures are promising fuel alternatives. Their HHVs are highly comparable to those of liquid transportation fuels (41-46 MJ kg^{-1}) [34]. Recently, plastic oils derived from polyolefins have been used as liquid fuels in various combustion systems [36,37].

Numerous researchers have attempted to directly produce value-added plastic oils from post-consumer waste materials. For example, different types of plastic mixtures have been used as reactants for plastic oil production via pyrolysis (Table 1). PE/PP/PS/PET mixtures present high yields of plastic oils (≥80%) [44,45] when slow pyrolysis is performed at ≤600 $^{\circ}$C. When plastic waste is composed

Table 1. Pyrolysis of polyolefins for producing fuel-range plastic oil

Plastic type	Reactor	Pyrolysis conditions	Catalyst	Plastic oil yield (wt%) including wax-like compound	Representative hydrocarbons involved in plastic oil	Refs.
LDPE	Fixed bed (multi-stage)	500 °C (10 °C min^{-1}, holding time: 20 min at 500 °C)	-	95	Oil: aliphatic C$_{9-50}$ HCs	[73]
			Y-zeolite 400 °C (catalyst bed temp.)	85 (gas: ~10)	Oil: aliphatic and aromatic HCs (such as toluene, ethylbenzene, xylenes, and PAHs) Gas: C$_{1-4}$ HCs	
			Y-zeolite 600 °C (catalyst bed temp.)	~70 (gas: ~20)		
			ZSM-5 400 °C (catalyst bed temp.)	88 (gas: ~5)		
			ZSM-5 600 °C (catalyst bed temp.)	~65 (gas: ~30)		
LDPE	Batch (single-stage fixed bed)	550 °C (5 °C min^{-1})	-	93.1 (gas: 14.6)	C$_{1-42}$ HCs	[74]
			HZSM5	18.3 (gas: 70.7)	C$_{1-18}$ HCs	
			HUSY	61.6 (gas: 34.5)	C$_{1-33}$ HCs	
HDPE			Absent	84.7 (gas: 16.3)	C$_{1-42}$ HCs	
			HZSM5	17.3 (gas: 72.6)	C$_{1-18}$ HCs	
			HUSY	41.0 (gas: 39.5)	C$_{1-33}$ HCs	
HDPE	Semi-batch (single stage)	420-510 °C (25 °C min^{-1})	FCC catalyst (SiO$_2$: 80.1%, Al$_2$O$_3$: 13.4%, Na: 0.3%, Ca: 1.5%, Fe 0.2%, V: 450 ppm, and Ni: 180 ppm)	89.1 (420 °C) 91.2 (450 °C) 85.3 (480 °C) 79.5 (510 °C)	C$_{5-9}$ olefins and paraffins	[75]
PP	Parr batch reactor	500 °C (5 °C min^{-1}, holding 1 h at 500 °C)	-	93 (gas: 7)	-	[76]
PP	Semi-batch (single stage)	420-510 °C (25 °C min^{-1})	FCC catalyst (SiO$_2$: 80.1%, Al$_2$O$_3$: 13.4%, Na: 0.3%, Ca: 1.5%, Fe 0.2%, V: 450 ppm, Ni: 180 ppm)	88.6 (420 °C) 92.3 (450 °C) 82.4 (480 °C) 76.1 (510 °C)	C$_{5-9}$ olefins, paraffins, and naphthenes	[77]
PP	Parr batch reactor	500 °C (5 °C min^{-1}, holding 1 h at 500 °C)	-	95 (gas: 5)	-	[76]
PS	Fixed bed (Multi-stage)	600 °C (10 °C min^{-1})	-	80.2 (gas: 19.8)	Styrene monomer, dimer, and trimer	[78]
			Ni/SiO$_2$ (600 °C)	76.6 (2% catalyst) 70.8 (5% catalyst) 61.8 (10% catalyst)		
PS	Parr batch reactor (Single-stage)	500 °C (5 °C min^{-1}, holding 1 h at 500 °C)	-	71 (gas: 2; residue: 27)	-	[76]
PS	Fixed bed	800 °C (350 °C min^{-1})	-	84.3 (gas: 5.7)	Naphthalene, fluorene, phenanthrene, anthracene, fluoranthene, and pyrene	[79]

Table 1. Continued

Plastic type	Reactor	Pyrolysis conditions	Catalyst	Plastic oil yield (wt%) including wax-like compound	Representative hydrocarbons involved in plastic oil	Refs.
PE (58.6), PP (26.9), PET (5.6), PS (8.8), Thermosets (0.1)	Batch (Single-stage)	500 °C (10 °C min⁻¹)	-	75.2 (gas: 14.2; residue: 10)	C_{5-14} HCs	[44]
		500 °C (20 °C min⁻¹)		82.2 (gas: 10.5; residue: 8.5)	$\geq C_{5-19}$ HCs	
		500 °C (20 °C ms⁻¹)		7 (gas: 91; residue: 2)	Gaseous HCs	
PE (45), PP (20), PS (20), PET (15)	Fluidized bed	600	-	81 (gas: 18, residue: 1.8)	Oil: $\geq C_5$ aliphatic and aromatic HCs	[45]
		700		46.8 (gas: 51, residue: 2.3)	Gas: CO, CO_2, C_{1-4} HCs	
HIPS (42.3), PMMA (32.1), ABS (21.2), PET (2.3), PC (2.2)	Fixed bed (Single-stage)	720 °C (10 °C min⁻¹)	-	72.1 (gas: 22.8, residue: 5.1)	Oil: Methyl methacrylate, bisphenol A, benzene derivatives, PAHs, styrene monomer, dimer, and trimer	[24]
	Fixed bed (Multi-stage)		600 °C (second heating stage temperature without catalyst)	49.0 (gas: 46.0, residue: 5.0)		
	Fixed bed (Multi-stage)		5 wt% Ni/SiO₂ (600 °C)	41.6 (gas: 53.3, residue: 5.1)	Gas: H_2, CO, CO_2, C_{1-2} HCs	

LDPE: low-density polyethylene, HDPE: high-density polyethylene, PP: polypropylene, PET: polyethylene terephthalate, PVC: polyvinyl chloride, PS: polystyrene, PA: Polyamide, HC: hydrocarbon, PAH: polyaromatic hydrocarbon; PE: polyethylene; PC: polycarbonate; HIPS: high impact polystyrene; PMMA: poly(methyl methacrylate); ABS: acrylonitrile butadiene styrene.

of up to 15 wt% of PET, HHV of the resulting plastic oil exceeds 41 MJ kg⁻¹ [46]. However, benzoic and terephthalic acids exist in plastic oil obtained from PET pyrolysis [47], and the combustion system can be damaged owing to the corrosiveness of the acid components. Therefore, additional post-treatment processes are essential to reduce the acidity of plastic oil derived from the practical post-consumer mixture. Moreover, the acid content in pyrolytic bio-oil is also problematic because biomass has a high oxygen content, which results in the high acidity of bio-oil [48]. Catalytic hydrodeoxygenation has long been employed to decrease oxygen content and acid functional groups [48,49]. Hydrogenolysis is one of the most widely used reactions to remove oxygen content with a supply of external hydrogen gas. In addition, CO_2-assisted pyrolysis has been employed to minimize the acid content in PET-derived plastic oil. When PET-containing waste is pyrolyzed, CO_2 reacts with plastic volatiles to simultaneously produce syngas and inhibit byproduct formation [41,50]. Barbarias et al. suggested multi-stage pyrolysis in-line catalytic steam reforming processes for hydrogen production instead of plastic oil production [51,52].

PVC contains highly reactive chlorine, which makes pyrolysis of PVC undesirable. Particularly, the thermal treatment of PVC is known to produce chlorinated hydrocarbons, which can cause problems in environmental and health issues [38,53]. For the removal of chlorine-containing chemicals from pyrolytic products, the use of an adsorbent before the combustion system is suggested [54,55].

To obtain high-purity plastic fuels, sorting polyolefins from other materials could be more favorable than the post-treatment of pyrolysis oils generated from a plastic waste mixture. As shown in Fig. 1, the densities of polyolefins and PET/PVC are significantly different, thereby facilitating the separation of polyolefins based on their density.

In addition to PE, PP, PS, PVC, and PET, other types of plastics are substantially present in plastic waste. Considering the pyrolysis of computer monitor waste, high-impact polystyrene (HIPS: 42.3%), polymethyl methacrylate (PMMA: 32.1%), and ABS (21.2%) are major plastic compounds in addition to low proportions of PET (2.3%) and polycarbonate (PC: 2.2%) [24]. Plastic oil derived from pyrolyzing the monitor waste contains substantial amounts of compounds, such as methyl methacrylate, benzene derivatives, PAHs, and bisphenol A with small amounts of fuel-range aliphatic HCs. Since the chemical composition of this plastic oil inhibits its use in liquid transportation fuels, further conversion into syngas is suggested [24].

2. Pyrolysis Gas from (Catalytic) Pyrolysis

Energy-intensive oils (HHVs $\geq$40 MJ kg⁻¹) can be produced from plastic pyrolysis. Polyolefins are considered suitable feedstocks for plastic oil production owing to their HHV and low level of impurities [42]. Therefore, the separation of polyolefins from the plastic waste stream is suggested to produce high-quality plastic liquid fuel.

In addition to producing plastic oil from polyolefins, other plastic
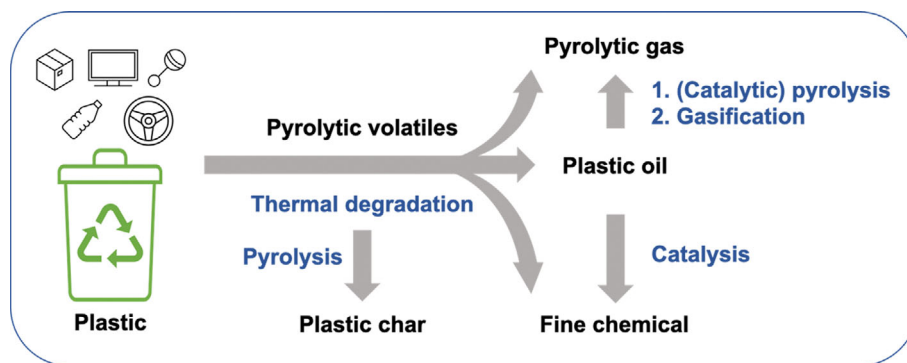
Fig. 3. Schematic of plastic waste management through different thermo-chemical processes.
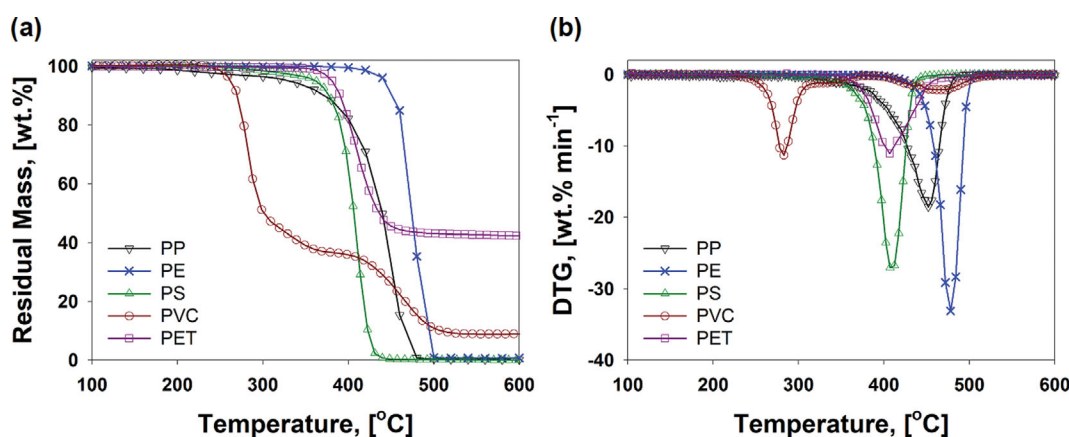

Fig. 4. Thermogravimetric analysis (TGA) of different plastics (PE [21,35], PP [80], PS [64], PVC [40], and PET [4]), comparing their (a) mass decay curve and (b) differential thermogram (DTG) curve as a function of temperature under N_2 condition (heating rate: $10\,^{o}C$ min^{-1}). Reprinted with permission from [6]. Copyright, Elsevier 2021.

waste mixtures can be valorized to obtain products such as syngas (H_2 and CO), which is a chemical intermediate used for the synthesis of value-added fuels and chemicals via Fischer-Tropsch reactions [56,57]. H_2 is also directly fed as a fuel for combustion [58] and fuel cell systems [59]. In addition, H_2 is used as a reductant for various industrial hydrogenation reactions [60-62].

Organic plastic waste can be thermally degraded into short-chained HCs, finally resulting in syngas (H_2 and CO) and CH_4 [63, 64]. Different pyrolytic volatiles can be converted to syngas at high-temperature regions with and without catalysts. Accordingly, different plastic waste mixtures are converted into syngas through gasification and catalytic pyrolysis.

Higher temperatures (700-1,000 ^{o}C) are required for gasification than for pyrolysis (≤700 ^{o}C) [65]. Gasification converts solid plastic waste to gaseous products through oxidation in the presence of oxidants such as air, steam, CO_2, or their mixtures [34,66]. Major gaseous products include syngas (H_2 and CO), CO_2, and C_{1-4} HCs. Catalytic pyrolysis involves chemical bond scissions of long-chain HCs over the catalyst surface. It has the advantage of requiring a lower working temperature than for gasification [67-69].

Previous attempts to produce syngas have involved the thermo-chemical upgrading of post-consumer plastic waste mixtures such as electronic and electrical equipment waste (E-waste) [5], tire waste

[70], and plastic-containing MSW [71,72]. Syngas is produced for the synthesis of longer chain HCs, which can also be directly obtained from the heterogeneous catalysis of postconsumer plastic as discussed in Section 4. The direct production of plastic oil and fine chemicals from thermo-chemical processes is more advantageous. Accordingly, the application of multiple chemical processes is proposed to maximize plastic waste valorization depending on the quality of the recovered plastic waste stream: (1) fine chemical production from high purity single plastics, (2) plastic fuel generation from polyolefins, and (3) syngas production from low-quality plastic mixtures (Fig. 3).

3. Applications of Plastic Solid Residue

Carbon-rich solid residues remain after the thermal degradation of plastic waste even at temperatures exceeding 900 ^{o}C (Fig. 4). The solid residue is known as plastic char. According to the thermogravimetric analysis (TGA) of different plastic types, PET and PVC provide high yields of plastic char after pyrolysis. Several pyrolysis studies have focused on the valorization of carbon materials obtained from plastic waste pyrolysis. Major applications include adsorbents for liquid and gaseous products.

Lee et al. developed activated carbons using different types of plastic such as PET [81-83] and PVC [84] for the adsorption of greenhouse gases (such as CH_4 and CO_2) and toxic chemical (including
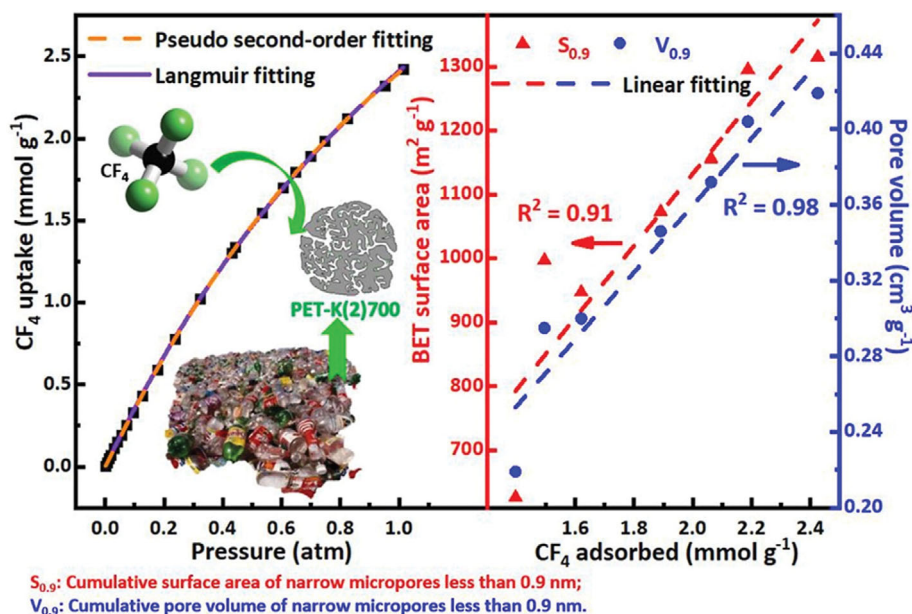
Fig. 5. CF_4 adsorption capacity of PET-derived plastic chars as a function of surface area and pore volume. Reprinted from [82] with permission. Copyright, Elsevier 2020.

CF_4). In the plastic-derived chars, micropores were formed through KOH activation, and N-containing functional groups were added through pyrolysis with urea. In general, the adsorption capacities of greenhouse and toxic gases were found to be proportional to the micropore volume, surface area, and the presence of N-containing functional groups [81-84]. The CF_4 adsorption capacity of PET bottle waste-derived plastic char based on the surface area, pore volume, and experimental condition is shown in Fig. 5.

Plastic waste-derived carbon materials were also developed for removing hazardous compounds from wastewater and toxic gas. Textile waste consists of PET and other additives such as flame retardants, wetting agents, and lubricants that cannot be separated easily [23]. Therefore, solid residues from textile waste pyrolysis are directly valorized into carbon materials to remove toxic compounds such as methylene blue dye, Cr(VI), iodine, phenol, and SO_2 [85-87]. Chemical activation methods are used to control the porosity of the functional carbon materials derived from plastic waste.

For instance, the adsorption capacities of carbon materials for toxic compounds such as iodine, methylene blue, and phenol (derived from PET fabric waste activated with ZnCl) are 896-1,060, 153-504, and 151-103 mg g^{-1}, respectively [88,89]. The methylene blue adsorption capacity of the plastic-derived carbon material is two orders of magnitude higher than that of adsorbents prepared from differently activated biochars [90-92].

HETEROGENEOUS CATALYSIS OF PLASTIC WASTE

Pyrolysis, which is the thermal degradation of plastic waste in the absence of oxygen, is commonly used to produce fuel-range chemicals (Section 3); however, this technique is hindered by low product selectivity and high operating temperatures (450-900 °C) [93]. In contrast, heterogeneous catalysis of plastic waste provides higher selectivity toward value-added products despite lower oper-

ating temperatures (200-300 °C). The presence of catalysts facilitates the selective cleavage of C-C bonds of PE and PP backbones; this is a crucial step in the production of targeted high-value-added products. Upcycling plastic waste into high-value-added chemicals via heterogeneous catalysis may provide economic incentives for plastic recycling, thus increasing environmental and economic sustainability and also the viability of a global circular economy.

1. Hydrogenolysis

High-value-added products have been extensively produced from plastic waste under mild conditions via catalytic hydrogenolysis, which involves the scission of C-C bonds over metal sites with H_2 [94-97]. Celik et al. reported that Pt on $SrTiO_3$ perovskite nanocuboids fabricated by atomic layer deposition completely convert PE samples into narrowly distributed high-quality liquid products, such as motor oil and waxes [94]. $Pt/SrTiO_3$ considerably suppresses excessive hydrogenolysis to light HCs (saturated C_1-C_8 and cyclic C_5-C_6), indicating that the performance of $Pt/SrTiO_3$ is superior to that of the commercial Pt/Al_2O_3 [94]. The selection of the support and metal significantly influences the reactivity in catalytic hydrogenolysis [96]. Among various metals (Ru, Ir, Rh, Pt, Pd Cu, Co, and Ni) and supports (CeO_2, TiO_2, MgO, ZrO_2, SiO_2, and H-USY), the activity of Ru/CeO_2 is considerably higher than those of other metal-supported catalysts for the hydrogenolysis of LDPE under mild conditions (200 °C and 2 MPa of H_2 pressure) [96]. Using Ru/CeO_2, various polyolefins such as LDPE, HDPE, and PP are converted to valuable chemicals in high yields (83-90%) owing to the selective cleavage of the internal C-C bonds in polyolefins, without isomerization or aromatization [96]. Moreover, the reaction rate (total metal basis) of Ru/CeO_2 is approximately 20-fold higher than that of previously reported $Pt/SrTiO_3$ catalyst, although the reaction temperature of Ru/CeO_2 (240 °C) is lower than that of $Pt/SrTiO_3$ (300 °C), as presented in Table 2 [96]. The reusability of Ru/CeO_2 was also tested at 240 °C for 8 h, and high conversion (>99%)

Table 2. Catalytic upcycling of plastic wastes

Reaction	Catalyst	Plastic type	Reaction conditions	Yield (%)		Note	Ref.
				Liquid	Wax		
Hydrogenolysis	Pt/SrTiO$_3$	HDPE	T=300 °C; P=11.7 bar; Time=96 h	97[a]			[94]
	Ru/C	PP	T=225 °C; P=40 bar; Time=24 h	ca. 35	-		[95]
	Ru/C	LDPE	T=225 °C; P=22 bar; Time=16 h	ca. 48	ca. 25		[110]
	Ru/C	HDPE	T=220 °C; P=30 bar; Time=1 h	74.9		n-pentane was used as a solvent	[99]
	Ru/CeO$_2$	LDPE	T=240 °C; P=35 bar; Time=18 h	82	5.4		[96]
	Ru/TiO$_2$	PP	T=250 °C; P=30 bar; Time=16 h	65.6	6.4		[111]
	Ru/WO$_3$/ZrO$_2$	LDPE	T=250 °C; P=50 bar; Time=2 h	ca. 47	ca. 15		[104]
	mSiO$_2$/Pt/SiO$_2$	HDPE	T=300 °C; P=14 bar; Time=24 h	78	0		[98]
Hydrocracking	Pt/WO$_3$/ZrO$_2$+HY	LDPE	T=250 °C; P=30 bar; Time=2 h	93	6		[97]
		PP	T=250 °C; P=30 bar; Time=2 h	ca. 81	0		
		HDPE	T=250 °C; P=30 bar; Time=2 h	ca. 73	0		
	Pt/WO$_3$/ZrO$_2$	LDPE	T=250 °C; P=30 bar; Time=12 h	78[b]	0		[103]
Tandem dehydrogenation and olefin metathesis	PtSn/Al$_2$O$_3$+ Re$_2$O$_7$/Al$_2$O$_3$	SRM-1475 (HDPE)	T=200 °C; P=40 bar (He); Time=15 h	ca. 72	ca. 6	n-pentane was used as a solvent	[107]
Tandem hydrogenolysis and aromatization	Pt/Al$_2$O$_3$		T=280 °C; P=1 bar; Time=12 h	71	17		[108]

[a]Yield is defined as the mass of the weight of hydrocarbons recovered relative to the initial mass of PE. [b]The liquid was considered to be C$_7$ or higher (Originally, the liquid was C$_5$ or higher, but the result of C$_4$-C$_6$ was bound and could not be separated.)

and yields toward liquid fuel and wax were maintained for five consecutive reactions.

More intricately designed catalysts mimicking the active site architecture of enzyme-catalyzed processes were employed for the hydrogenolysis of HDPE to obtain a narrow distribution of diesel and lubricant-range alkanes (C$_9$-C$_{18}$) [98]. Pt nanoparticles located at the base of silica mesopores in mesoporous shell/active site/core (mSiO$_2$/Pt/SiO$_2$) catalyst could facilitate a processive catalytic mechanism, wherein polyolefins are not released from the pores, but short-chain products are allowed to escape [98]. Thus, the HC chains obtained using mSiO$_2$/Pt/SiO$_2$ appear as a bell-curve distribution of chain lengths, centered at C$_{14}$ comprising 40% of the HCs. In contrast, HDPE chains were randomly cleaved over fully exposed Pt nanoparticles in Pt/SiO$_2$, resulting in a flattened distribution of HC chains with carbon values ranging from C$_{18}$ to C$_{26}$. (5.8±0.2% for each species) [98]. In addition to the abovementioned modifications of active metals, supports, and catalyst structure, solvents have been found to promote hydrogenolysis activity. Jia et al. demonstrated that the commercial Ru/C catalyst converts 90 wt% HDPE to C$_{8+}$ liquid HC products within only 1 h under mild conditions (30 bar H$_2$ and 220 °C) in the presence of the solvent n-hexane [99]. The molecular dynamics simulations suggest that the interaction between PE polymers and solvent molecules changes the con-

formation of the PE polymer, thereby influencing the hydrogenolysis reaction kinetics and product selectivity [99]. The use of non-polar linear HC solvents, particularly linear alkanes such as n-hexane, considerably reduces the reaction time (1 h) compared with that of other solvent-free systems (>6 h).

Most catalytic systems for catalytic conversion of polyolefins currently depend on high loadings (≥5 wt%) of precious metal catalysts such as Ru and Pt; however, the high cost and low availability of precious metals have prompted the shift from high to low loadings of precious metals or from precious to non-precious metals. Chen et al. reported that low-loading (≤0.25%) Ru/CeO$_2$ catalysts exhibit a superior hydrogenolysis rate per surface Ru than high-loading (≥0.5%) Ru/CeO$_2$ catalysts [100]. The intrinsic activity of Ru in PP and LDPE hydrogenolysis increases with decreasing particle size in the low Ru loading range, in contrast to that in the high-loading range [100]. Based on X-ray photoelectron spectroscopy and in situ extended X-ray absorption fine structure results, abrupt changes in catalytic behavior are associated with Ru species transitioning from well-defined to highly disordered structures in the low-loading range [100]. The enhanced activity of low-loading Ru/CeO$_2$ was ascribed to the higher coverage of adsorbed hydrogen (*H), which regulated the regioselectivity by favoring the cleavage of C-C bonds involving less hydrogenated transition states (includ-
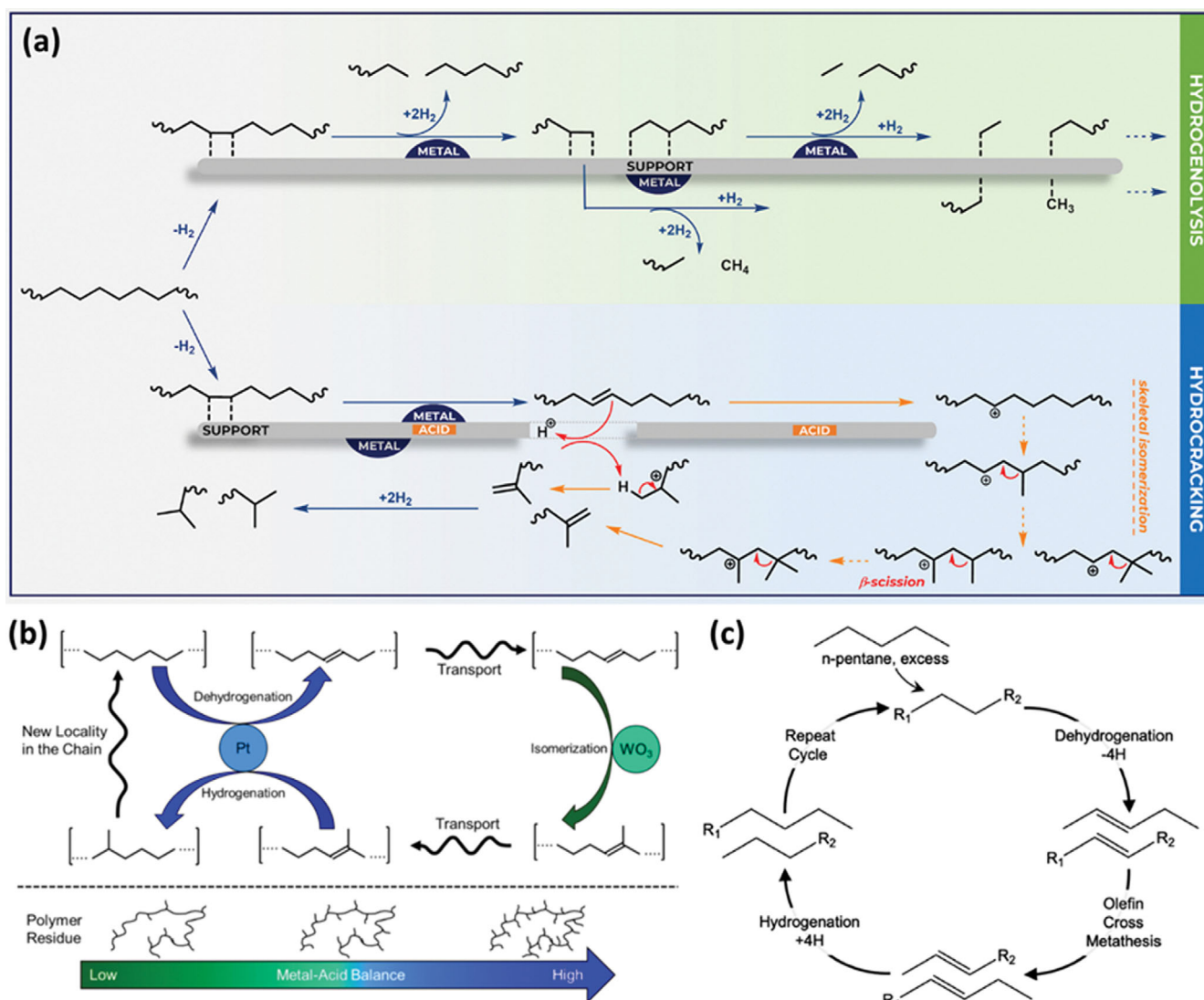
Fig. 6. (a) Hydrogenolysis and hydrocracking reaction mechanisms. Reprinted with permission from ref [109]. Copyright 2022 Elsevier. (b) Effect of the metal-acid balance on the isomerization cycle during LDPE hydrocracking. Reprinted with permission from ref [103]. Copyright 2021 Elsevier. (c) Tandem dehydrogenation and olefin cross metathesis (TDOCM) reaction mechanism. Reprinted with permission from ref [107]. Copyright 2021 American Chemical Society.

ing internal rather than terminal C-C bonds), and branching C-C bonds in LDPE [100]. Instead of using noble metal catalysts, non-precious Co (5 wt%) supported on ZSM-5 zeolite efficiently catalyzed the solvent-free hydrogenolysis of PE and PP into propane with high selectivity ($\geq$80 wt%) under mild conditions (250 °C and 40 bar H_2 in 20 h) as demonstrated by Zichittella and et al. [101]. Co/ZSM-5 catalyst substantially reduced the formation of the undesired CH_4 product ($\leq$5 wt%) because highly dispersed oxidic cobalt nanoparticles were stabilized by the zeolite [101]. By preventing complete reduction to metallic species and/or formation of large clusters, the stabilized oxidic CO nanoparticles on ZSM-5 could selectively produce propane while suppressing CH_4 formation [101]. The high selectivity toward propane was only observed over Co/ZSM-5, and not bulk Co_3O_4, or other cobalt-based systems supported on other carriers [101]. Other catalytic systems are summarized for comparision in Table 2.

2. Hydrocracking

In the hydrogenolysis reaction, both C-H bond activation and C-C bond cleavage occur at metal sites, whereas in the hydrocracking process, the C-H bond activation and C-C bond cracking occur at metal and acid sites, respectively (Fig. 6(a)). Thus, bifunctional catalysts consisting of metal (Pt, Pd, and Ni) and acid sites have been employed for polyolefin hydrocracking [97,102,103]. In contrast to hydrogenolysis, which easily leads to over-cracking that results in low-value gases (C_1-C_3), hydrocracking suppresses light gas generation and produces highly isomerized products (higher value branched fuel- and lubricant-ranged alkanes) [97,103] Liu et al. reported that Pt/WO_3/ZrO_2 and HY zeolite selectively convert polyolefins to highly branched gasoline or jet and diesel-range HC products with a high yield (up to 85%) via bifunctional metal-acid mechanism under mild conditions (250 °C and 30 bar H_2 in 2 h) [97]. The reaction was performed in tandem catalysis with the poly-

olefins initially being activated over Pt, followed by cracking over the acid sites of the WO_3/ZrO_2 and HY zeolite, isomerization over the WO_3/ZrO_2 sites, and hydrogenation of intermediate olefins over Pt. Compared with monofunctional hydrogenolysis, bifunctional tandem catalysis allows more rapid polymer conversion and fine-tuning of the activity and selectivity [97].

In a follow-up study, Vance et al. observed the relationship between the catalyst metal-to-acid balance (MAB) and the hydrocracking mechanism in $Pt/WO_3/ZrO_2$ catalysts [103]. At a high MAB, dehydrogenation was facilitated on metal sites, whereas the acid-catalyzed C-C bond cracking was relatively slow, increasing the isomerization degree in the residual polymer (Fig. 6(b)) [103]. Owing to the bifunctionality, MAB over various $Pt/WO_3/ZrO_2$ catalysts was found to be controlled to produce branched, high-value products such as lubricant oils rather than light gases in the LDPE hydrocracking. In contrast, when the $Ru/WO_x/ZrO_2$ catalysts were employed for LDPE depolymerization instead of $Pt/WO_3/ZrO_2$, negligible isomerization activity was observed, indicating the absence of metal-acid bifunctional hydrocracking-isomerization chemistry [104]. The bifunctional $Pt/WO_3/ZrO_2$ catalysts promote a high degree of branching, whereas Ru in $Ru/WO_x/ZrO_2$ catalysts facilitates dehydrogenation and subsequent C-C scission while inhibiting hydrocracking and isomerization over the Brønsted acid sites [104]. This indicates the presence of acid sites in $Ru/WO_x/ZrO_2$ catalysts is not considerably crucial to suppressing methane production.

3. Tandem Catalysis

A tandem dehydrogenation and olefin cross metathesis (TDOCM) reaction can break down PE into liquid fuels and waxes under mild conditions. In contrast to hydrogenolysis and hydrocracking, the TDOCM reaction proceeds without an external H_2 supply. TDOCM was originally used for alkane metathesis via a tandem catalytic system consisting of an Ir complex and a Schrock-type catalyst [105]. A homogeneous Ir complex was found to be active for alkane dehydrogenation and olefin hydrogenation, whereas with the Schrock-type catalyst, the chemical functionalities of two olefins could be rearranged via metathesis [105]. TDOCM facilitates olefin metathesis rearrangements using alkane substrates unlike conventional olefin metathesis that uses alkene substrates. The TDOCM reaction consists of three reaction steps: (1) dehydrogenation of alkane (paraffin) to alkene, (2) alkene (olefin) metathesis, and (3) hydrogenation of alkene to alkane [105], as shown in Fig. 6(c). Recently, the TDOCM reaction was introduced to depolymerize PE into valuable liquid fuels or chemical feedstocks. Jia et al. investigated the TDOCM reaction between PE and a light alkane such as n-octane or n-hexane using various Al_2O_3-supported Ir complexes for dehydrogenation and hydrogenation with a heterogeneous Re_2O_7/Al_2O_3 catalyst for olefin metathesis [106]. The TDOCM system efficiently degrades PE; consequently, 51-85% of PE is converted to oil products depending on the type of PE (such as HDPE, LDPE, LLDPE, and PE) under mild reaction conditions (150-175 °C and atmospheric pressure) [106]. Ellis et al. proposed a completely heterogeneous TDOCM system consisting of a physical mixture of $PtSn/Al_2O_3$ and Re_2O_7/Al_2O_3 for tandem dehydrogenation and olefin metathesis, respectively [107]. The molecular weight of HDPE was observed to decrease by 73% after 15 h reaction under mild conditions (200 °C and atmospheric pressure) [107]. Despite the

milder reaction conditions relative to hydrogenolysis and hydrocracking processes, the active reaction temperature of the two catalysts is different; thus, the TDOCM reaction has a narrow operation temperature window. The Pt-based catalyst is not active for alkane dehydrogenation at low reaction temperature, whereas the Re-based olefin metathesis catalysts are unstable at the high reaction temperature.

Instead of producing alkanes via the abovementioned approaches, Zhang et al. proposed the production of high-value aromatics from PE. PE could be upcycled into high-value long-chain alkyl-aromatics via tandem hydrogenolysis and aromatization using Pt/Al_2O_3 without consuming the external H_2 [108]. According to theoretical calculation, 90% of H_2 produced from the dehydro-aromatization reaction of shorter HC chains is consumed during hydrogenolysis [108]. In addition, the integration of exothermic hydrogenolysis and endothermic aromatization decreases the overall reaction temperature (280 °C) [108]. The conversion of commercial LDPE bags and HDPE water-bottle caps using a tandem catalytic system provides high yields of 69 and 55 wt% with alkyl-aromatic selectivity of 44 and 50%, respectively, thus validating the application of tandem hydrogenolysis and aromatization for producing high-value aromatics from plastic wastes. Moreover, the stability of the Pt/Al_2O_3 catalyst was tested by conducting three consecutive reactions, and a decrease in the liquid/wax yield (15 wt%) was observed in the second run and stabilized in the third run. However, the turnover frequency remains the same, indicating that the intrinsic activity of the catalyst appears to be unchanged between each experiment.

CONCLUSIONS AND PERSPECTIVES

Thus far, we have discussed various existing plastic waste upcycling strategies such as (catalytic) pyrolysis and heterogeneous catalysis. In contrast to heterogeneous catalysis, the technical readiness of the pyrolysis process allows different types of plastic mixtures to be simultaneously depolymerized, which is advantageous, considering the nature of post-consumer plastic waste that contains heterogeneous mixtures. Simultaneous depolymerization reduces the separation and sorting processes of plastic mixtures. The thermal process, such as (catalytic) pyrolysis, has been scaled up to the commercial level. However, additional efforts are needed to develop a commercial-scale technology for upcycling plastic mixtures via heterogeneous catalysis.

In addition, heterogeneous catalysis involves multiple types of catalytic processes; thus, the upcycling efficiency can be improved through the identification of active sites and reaction mechanisms [112]. For example, catalytic activity in alkane hydrogenolysis is known to be sensitive to structures (geometric and electronic), supports, and promoters; therefore, the influence of those parameters on the plastic waste upcycling process must be examined [113-115]. Moreover, further studies are necessary to elucidate the role of solvents in heterogeneous catalysis. Although the presence of solvents has been found to significantly promote hydrogenolysis activity (Section 4.1), the influence of solvents on the catalytic properties has not been comprehensively investigated. The role of solvents must be clarified in terms of (i) interaction between substrate and solvent, (ii) substrate conformation, and (iii) kinetics and heat/mass

transfer.

In addition to the optimal design of catalysts, combining the existing thermo-chemical "upcycling" processes with other reactions may be an efficient and sustainable strategy to upcycle plastic waste. For example, Liu et al. proposed an efficient solar thermal catalysis to recycle various polyesters into high-value-added monomer derivatives with low energy consumption and carbon emissions [116]. Compared with traditional thermal catalysis, the recycling efficiency of the solar thermal process is three times higher at a lower depolymerization temperature. Furthermore, compared with thermal catalysis, the solar thermal process can reduce energy consumption by 3.7 GJ and CO_2 emissions by 0.4 tons per ton of polyester. In addition, Li et al. enhanced PET depolymerization by combining it with CO_2 hydrogenation [117]. The dual-promoted conversion processes involving CO_2 hydrogenation and PET methanolysis overcome the original thermodynamic equilibrium limits of methanol synthesis, thus significantly enhancing PET depolymerization. This synergistic catalytic process provides an effective way to simultaneously upcycle two wastes, namely, polyesters, and CO_2, for producing high-value chemicals.

Through this review, we discussed the opportunities of various existing plastic waste upcycling strategies. The major challenges of the existing plastic waste upcycling strategies are (i) heat and mass transfer limitations, and (ii) catalyst deactivation during post-consumer plastic waste. Heat and mass transfer limitations occur often in existing plastic waste upcycling strategies such as (catalytic) pyrolysis and heterogeneous catalysis. Heat and mass transfer facilitation provides shorter reaction timescales and higher selectivity at lower reaction temperatures; thus, extensive work (i.e., novel catalyst design and reactor engineering) is necessary to overcome those issues. Another challenge is catalyst deactivation by coke and poisoning. Coke formation decreases the overall reaction efficiency and lifetime of the catalyst, thereby increasing the overall operating cost. Thus, long-term stability of the catalyst must be achieved in future works (i.e., developing coke-resistant catalysts and optimal operating conditions) In addition to coke, the presence of impurities such as heteroatomic compounds and metals present in plastic waste may poison catalysts, thereby decreasing the reactivity of catalysts. For example, nitrogen is present in some plastics, such as nylon (polyamide) and ABS plastic (polyaniline), which may poison catalysts and influence catalyst stability. The presence of those impurities is, indeed, generally detrimental to catalyst performance. However, a recent study found that metal impurities such as Fe, Ni, and V enhance aromatics selectivity and suppress coke formation in the catalytic cracking of PP using industrial FCC catalysts [118]. Thus, it is worth investigating the effect of impurities in plastic waste on the performance and stability of the catalysts in future studies.

ACKNOWLEDGEMENT

REFERENCES

1. S. Thakur, A. Verma, B. Sharma, J. Chaudhary, S. Tamulevicius and V. K. Thakur, *Curr. Opin. Green Sustain. Chem.*, **13**, 32 (2018).
2. K. J. Groh, T. Backhaus, B. Carney-Almroth, B. Geueke, P. A. Inostroza, A. Lennquist, H. A. Leslie, M. Maffini, D. Slunge, L. Trasande, A. M. Warhurst and J. Muncke, *Sci. Total Environ.*, **651**, 3253 (2019).
3. R. H. Faraj, H. F. Hama Ali, A. F. H. Sherwani, B. R. Hassan and H. Karim, *J. Build. Eng.*, **30**, 101283 (2020).
4. D. Kwon, S. Yi, S. Jung and E. E. Kwon, *Environ. Pollut.*, **268**, 115916 (2021).
5. J. Joo, E. E. Kwon and J. Lee, *Environ. Pollut.*, **287**, 117621 (2021).
6. S. Jung, S.-H. Cho, K.-H. Kim and E. E. Kwon, *Chem. Eng. J.*, **422**, 130154 (2021).
7. OECD, Global Plastics Outlook (2022).
8. G. Iaquaniello, G. Centi, A. Salladini, E. Palo, S. Perathoner and L. Spadaccini, *Bioresour. Technol.*, **243**, 611 (2017).
9. J. N. Hahladakis and E. Iacovidou, *Sci. Total Environ.*, **630**, 1394 (2018).
10. A. L. P. Silva, J. C. Prata, A. C. Duarte, A. M. V. M. Soares, D. Barceló and T. Rocha-Santos, *Case Stud. Therm. Eng.*, **3**, 100072 (2021).
11. S. Dobaradaran, T. C. Schmidt, N. Lorenzo-Parodi, W. Kaziur-Cegla, M. A. Jochmann, I. Nabipour, H. V. Lutze and U. Telgheder, *Environ. Pollut.*, **259**, 113916 (2020).
12. C.-T. Li, H.-K. Zhuang, L.-T. Hsieh, W.-J. Lee and M.-C. Tsao, *Environ. Int.*, **27**, 61 (2001).
13. J. Dong, Y. Tang, A. Nzihou, Y. Chi, E. Weiss-Hortala and M. Ni, *Sci. Total Environ.*, **626**, 744 (2018).
14. F. Wakefield, Top 25 recycling facts and statistics for 2022, in, World Economic Forum (2022).
15. Y.-C. Jang, G. Lee, Y. Kwon, J.-h. Lim and J.-h. Jeong, *Resour. Conserv. Recycl.*, **158**, 104798 (2020).
16. J. Di, B. K. Reck, A. Miatto and T. E. Graedel, *Resour. Conserv. Recycl.*, **167**, 105440 (2021).
17. G. Faraca and T. Astrup, *Waste Manag.*, **95**, 388 (2019).
18. X. Chen, Y. Wang and L. Zhang, *ChemSusChem*, **14**, 4137 (2021).
19. J. Lee, E. E. Kwon, S. S. Lam, W.-H. Chen, J. Rinklebe and Y.-K. Park, *J. Clean. Prod.*, **321**, 128989 (2021).
20. L. O. Mark, M. C. Cendejas and I. Hermans, *ChemSusChem*, **13**, 5808 (2020).
21. S. Jung, D. Choi, Y.-K. Park, Y. F. Tsang, N. B. Klinghoffer, K.-H. Kim and E. E. Kwon, *Chem. Eng. J.*, **399**, 125889 (2020).
22. P. M. Subramanian, *Resour. Conserv. Recycl.*, **28**, 253 (2000).
23. S. Ügdüler, K. M. Van Geem, M. Roosen, E. I. P. Delbeke and S. De Meester, *Waste Manag.*, **104**, 148 (2020).
24. S. Jung, S. Lee, H. Song, Y. F. Tsang and E. E. Kwon, *ACS Sustain. Chem. Eng.*, **10**, 8443 (2022).
25. S. Serranti and G. Bonifazi, 2 - Techniques for separation of plastic wastes, in: F. Pacheco-Torgal, J. Khatib, F. Colangelo, R. Tuladhar (Eds.) Use of Recycled Plastics in Eco-efficient Concrete, Woodhead Publishing, 9 (2019).
26. Omnexus, Density of Plastics: Technical Properties, in, Paris, France (2022).
27. Y. W. Huang, M. Q. Chen, Q. H. Li and W. Xing, *Energy*, **156**, 548 (2018).
28. G. Dodbiba, A. Shibayama, T. Miyazaki and T. Fujita, *Magn. Electr. Sep.*, **11**, 096372 (2002).
29. E. J. Bakker, P. C. Rem and N. Fraunholcz, *Waste Manag.*, **29**, 1712 (2009).

30. S. Serranti, V. Luciani, G. Bonifazi, B. Hu and P. C. Rem, *Waste Manag.*, **35**, 12 (2015).

31. M. Roosen, L. Harinck, S. Ügdüler, T. De Somer, A.-G. Hucks, T. G. A. Belé, A. Buettner, K. Ragaert, K. M. Van Geem, A. Dumoulin and S. De Meester, *Sci. Total Environ.*, **812**, 152467 (2022).

32. L. Cutroneo, A. Reboa, G. Besio, F. Borgogno, L. Canesi, S. Canuto, M. Dara, F. Enrile, I. Forioso, G. Greco, V. Lenoble, A. Malatesta, S. Mounier, M. Petrillo, R. Rovetta, A. Stocchino, J. Tesan, G. Vagge and M. Capello, *Environ. Sci. Pollut Res.*, **27**, 8938 (2020).

33. S. B. Lee, J. Lee, Y. F. Tsang, Y.-M. Kim, J. Jae, S.-C. Jung and Y.-K. Park, *Environ. Pollut.*, **283**, 117060 (2021).

34. A. Antelava, N. Jablonska, A. Constantinou, G. Manos, S. A. Salaudeen, A. Dutta and S. M. Al-Salem, *Energy Fuels*, **35**, 3558 (2021).

35. D. Choi, S. Jung, S. S. Lee, K.-Y. A. Lin, Y.-K. Park, H. Kim, Y. F. Tsang and E. E. Kwon, *Renew. Sustain. Energy Rev.*, **138**, 110559 (2021).

36. S. Wang, H. Kim, D. Lee, Y.-R. Lee, Y. Won, B. W. Hwang, H. Nam, H.-J. Ryu and K.-H. Lee, *Fuel*, **305**, 121440 (2021).

37. S. Wang, D. A. Rodriguez Alejandro, H. Kim, J.-Y. Kim, Y.-R. Lee, W. Nabgan, B. W. Hwang, D. Lee, H. Nam and H.-J. Ryu, *Energy*, **247**, 123408 (2022).

38. J. Yu, L. Sun, C. Ma, Y. Qiao and H. Yao, *Waste Manag.*, **48**, 300 (2016).

39. H. M. Zhu, X. G. Jiang, J. H. Yan, Y. Chi and K. F. Cen, *J. Anal. Appl. Pyrol.*, **82**, 1 (2008).

40. T. Lee, J.-I. Oh, K. Baek, Y. F. Tsang, K.-H. Kim and E. E. Kwon, *Green Chem.*, **20**, 1583 (2018).

41. D. Kwon, S. Jung, D. H. Moon, Y. F. Tsang, W.-H. Chen and E. E. Kwon, *Chem. Eng. J.*, **437**, 135524 (2022).

42. B. Kunwar, H. N. Cheng, S. R. Chandrashekaran and B. K. Sharma, *Renew. Sustain. Energy Rev.*, **54**, 421 (2016).

43. S. Jung, J.-M. Jung, K. H. Lee and E. E. Kwon, *Energy Convers. Manag.*, **244**, 114479 (2021).

44. R. K. Singh, B. Ruj, A. K. Sadhukhan and P. Gupta, *J. Energy Inst.*, **92**, 1647 (2019).

45. G. Grause, S. Matsumoto, T. Kameda and T. Yoshioka, *Ind. Eng. Chem. Res.*, **50**, 5459 (2011).

46. R. Miandad, M. A. Barakat, A. S. Aburiazaiza, M. Rehan, I. M. I. Ismail and A. S. Nizami, *Int. Biodeterior. Biodegrad.*, **119**, 239 (2017).

47. L. S. Diaz-Silvarrey, A. McMahon and A. N. Phan, *J. Anal. Appl. Pyrol.*, **134**, 621 (2018).

48. H. Lee, Y.-M. Kim, I.-G. Lee, J.-K. Jeon, S.-C. Jung, J. D. Chung, W. G. Choi and Y.-K. Park, *Korean J. Chem. Eng.*, **33**, 3299 (2016).

49. S. Kim, E. E. Kwon, Y. T. Kim, S. Jung, H. J. Kim, G. W. Huber and J. Lee, *Green Chem.*, **21**, 3715 (2019).

50. J. Lee, T. Lee, Y. F. Tsang, J.-I. Oh and E. E. Kwon, *Energy Convers. Manag.*, **148**, 456 (2017).

51. I. Barbarias, G. Lopez, M. Artetxe, A. Arregi, J. Bilbao and M. Olazar, *Energy Convers. Manag.*, **156**, 575 (2018).

52. I. Barbarias, G. Lopez, M. Amutio, M. Artetxe, J. Alvarez, A. Arregi, J. Bilbao and M. Olazar, *Appl. Catal. A: Gen.*, **527**, 152 (2016).

53. S. Rezania, B. Oryani, J. Park, B. Hashemi, K. K. Yadav, E. E. Kwon, J. Hur and J. Cho, *Energy Convers. Manag.*, **201**, 112155 (2019).

54. M. F. Ali and M. N. Siddiqui, *J. Anal. Appl. Pyrol.*, **74**, 282 (2005).

55. A. Lopez-Urionabarrenechea, I. de Marco, B. M. Caballero, M. F. Laresgoiti and A. Adrados, *J. Anal. Appl. Pyrol.*, **96**, 54 (2012).

56. A. Corma, S. Iborra and A. Velty, *Chem. Rev.*, **107**, 2411 (2007).

57. K. Fang, D. Li, M. Lin, M. Xiang, W. Wei and Y. Sun, *Catal. Today*, **147**, 133 (2009).

58. M. Winter and R. J. Brodd, *Chem. Rev.*, **104**, 4245 (2004).

59. M. W. Ellis, M. R. V. Spakovsky and D. J. Nelson, *Proc. IEEE*, **89**, 1808 (2001).

60. A. S. May and E. J. Biddinger, *ACS Catal.*, **10**, 3212 (2020).

61. G. W. Huber, S. Iborra and A. Corma, *Chem. Rev.*, **106**, 4044 (2006).

62. R.-P. Ye, J. Ding, W. Gong, M. D. Argyle, Q. Zhong, Y. Wang, C. K. Russell, Z. Xu, A. G. Russell, Q. Li, M. Fan and Y.-G. Yao, *Nat. Commun.*, **10**, 5698 (2019).

63. S. Zhang, S. Zhu, H. Zhang, X. Liu and Y. Xiong, *Int. J. Hydrog. Energy*, **44**, 26193 (2019).

64. T. Lee, S. Jung, Y.-K. Park, T. Kim, H. Wang, D. H. Moon and E. E. Kwon, *J. Hazard. Mater.*, **395**, 122576 (2020).

65. W.-J. Liu, H. Jiang and H.-Q. Yu, *Chem. Rev.*, **115**, 12251 (2015).

66. G. Lopez, M. Artetxe, M. Amutio, J. Alvarez, J. Bilbao and M. Olazar, *Renew. Sustain. Energy Rev.*, **82**, 576 (2018).

67. E. E. Kwon, S. Kim and J. Lee, *J. CO₂ Util.*, **31**, 173 (2019).

68. J. M. Saad and P. T. Williams, *Waste Manag.*, **58**, 214 (2016).

69. J. M. Saad and P. T. Williams, *Energy Fuels*, **30**, 3198 (2016).

70. Y. Pan, X. Du, C. Zhu, J. Wang, J. Xu, Y. Zhou and Q. Huang, *Int. J. Hydrog. Energy*, **47**, 33966 (2022).

71. Q. Zhang, L. Dor, A. K. Biswas, W. Yang and W. Blasiak, *Fuel Process. Technol.*, **106**, 546 (2013).

72. S. M. Al-Salem, A. Antelava, A. Constantinou, G. Manos and A. Dutta, *J. Environ. Manage.*, **197**, 177 (2017).

73. R. Bagri and P. T. Williams, *J. Anal. Appl. Pyrol.*, **63**, 29 (2002).

74. A. Marcilla, M. I. Beltrán and R. Navarro, *Appl. Catal. B: Environ.*, **86**, 78 (2009).

75. M. S. Abbas-Abadi, M. N. Haghighi and H. Yeganeh, *Fuel Process. Technol.*, **109**, 90 (2013).

76. P. T. Williams and E. Slaney, *Resour. Conserv. Recycl.*, **51**, 754 (2007).

77. M. S. Abbas-Abadi, M. N. Haghighi, H. Yeganeh and A. G. McDonald, *J. Anal. Appl. Pyrol.*, **109**, 272 (2014).

78. D. Choi, S. Jung, Y. F. Tsang, H. Song, D. H. Moon and E. E. Kwon, *Sci. Total Environ.*, **834**, 155384 (2022).

79. H. Zhou, C. Wu, J. A. Onwudili, A. Meng, Y. Zhang and P. T. Williams, *Waste Manag.*, **36**, 136 (2015).

80. S. Jung, S. Lee, X. Dou and E. E. Kwon, *Chem. Eng. J.*, **405**, 126658 (2021).

81. X. Yuan, S. Li, S. Jeon, S. Deng, L. Zhao and K. B. Lee, *J. Hazard. Mater.*, **399**, 123010 (2020).

82. X. Yuan, M.-K. Cho, J. G. Lee, S. W. Choi and K. B. Lee, *Environ. Pollut.*, **265**, 114868 (2020).

83. X. Yuan, J. G. Lee, H. Yun, S. Deng, Y. J. Kim, J. Lee, S. K. Kwak and K. B. Lee, *Chem. Eng. J.*, **397**, 125350 (2020).

84. H. I. Park, J. Kang, J.-H. Park, J. C. Park, J. Park, K. B. Lee and C. H. Lee, *Chem. Eng. J.*, **440**, 135867 (2022).

85. Z. Xu, D. Zhang, Z. Yuan, W. Chen, T. Zhang, D. Tian and H. Deng, *Environ. Sci. Pollut. Res.*, **24**, 22602 (2017).

86. W. Chen, Y. Zhang, S. Zhang, W. Lu and H. Xu, *Waste Biomass Valor.*, **11**, 4259 (2020).

87. J. M. Illingworth, B. Rand and P. T. Williams, *Process Saf. Environ. Prot.*, **122**, 209 (2019).

88. X. Yu, S. Wang and J. Zhang, *J. Mater. Sci.*, **53**, 5458 (2018).

89. X. Yu, S. Wang, Y. Gao and Z. Bao, *Environ. Sci. Pollut. Res.*, **25**, 30567 (2018).

90. G. Ding, B. Wang, L. Chen and S. Zhao, *Chemosphere*, **163**, 283 (2016).

91. L. Sun, S. Wan and W. Luo, *Bioresour. Technol.*, **140**, 406 (2013).

92. J.-H. Park, J. J. Wang, Y. Meng, Z. Wei, R. D. DeLaune and D.-C. Seo, *Colloids Surf. A: Physicochem. Eng. Asp.*, **572**, 274 (2019).

93. D. Zhao, X. Wang, J. B. Miller and G. W. Huber, *ChemSusChem*, **13**, 1764 (2020).

94. G. Celik, R. M. Kennedy, R. A. Hackler, M. Ferrandon, A. Tennakoon, S. Patnaik, A. M. LaPointe, S. C. Ammal, A. Heyden, F. A. Perras, M. Pruski, S. L. Scott, K. R. Poeppelmeier, A. D. Sadow and M. Delferro, *ACS Cent. Sci.*, **5**, 1795 (2019).

95. J. E. Rorrer, C. Troyano-Valls, G. T. Beckham and Y. Román-Leshkov, *ACS Sustain. Chem. Eng.*, **9**, 11661 (2021).

96. Y. Nakaji, M. Tamura, S. Miyaoka, S. Kumagai, M. Tanji, Y. Nakagawa, T. Yoshioka and K. Tomishige, *Appl. Catal. B: Environ.*, **285**, 119805 (2021).

97. S. Liu, P. A. Kots, B. C. Vance, A. Danielson and D. G. Vlachos, *Sci. Adv.*, **7**, eabf8283 (2021).

98. A. Tennakoon, X. Wu, A. L. Paterson, S. Patnaik, Y. Pei, A. M. LaPointe, S. C. Ammal, R. A. Hackler, A. Heyden, I. I. Slowing, G. W. Coates, M. Delferro, B. Peters, W. Huang, A. D. Sadow and F. A. Perras, *Nat. Catal.*, **3**, 893 (2020).

99. C. Jia, S. Xie, W. Zhang, N. N. Intan, J. Sampath, J. Pfaendtner and H. Lin, *Chem. Catal.*, **1**, 437 (2021).

100. L. Chen, L. C. Meyer, L. Kovarik, D. Meira, X. I. Pereira-Hernandez, H. Shi, K. Khivantsev, O. Y. Gutiérrez and J. Szanyi, *ACS Catal.*, **12**, 4618 (2022).

101. G. Zichittella, A. M. Ebrahim, J. Zhu, A. E. Brenner, G. Drake, G. T. Beckham, S. R. Bare, J. E. Rorrer and Y. Román-Leshkov, *JACS Au*, **2**, 2259 (2022).

102. W. Ding, J. Liang and L. L. Anderson, *Energy Fuels*, **11**, 1219 (1997).

103. B. C. Vance, P. A. Kots, C. Wang, Z. R. Hinton, C. M. Quinn, T. H. Epps, L. T. J. Korley and D. G. Vlachos, *Appl. Catal. B: Environ.*, **299**, 120483 (2021).

104. C. Wang, T. Xie, P. A. Kots, B. C. Vance, K. Yu, P. Kumar, J. Fu, S. Liu, G. Tsilomelekis, E. A. Stach, W. Zheng and D. G. Vlachos, *JACS Au*, **1**, 1422 (2021).

105. A. S. Goldman, A. H. Roy, Z. Huang, R. Ahuja, W. Schinski and M. Brookhart, *Science*, **312**, 257 (2006).

106. X. Jia, C. Qin, T. Friedberger, Z. Guan and Z. Huang, *Sci. Adv.*, **2**, e1501591 (2016).

107. L. D. Ellis, S. V. Orski, G. A. Kenlaw, A. G. Norman, K. L. Beers, Y. Román-Leshkov and G. T. Beckham, *ACS Sustain. Chem. Eng.*,

108. F. Zhang, M. Zeng, R. D. Yappert, J. Sun, Y.-H. Lee, A. M. LaPointe, B. Peters, M. M. Abu-Omar and S. L. Scott, *Science*, **370**, 437 (2020).

109. A. Piovano and E. Paone, *Curr. Res. Green Sustain. Chem.*, **5**, 100334 (2022).

110. J. E. Rorrer, G. T. Beckham and Y. Román-Leshkov, *JACS Au*, **1**, 8 (2021).

111. P. A. Kots, S. Liu, B. C. Vance, C. Wang, J. D. Sheehan and D. G. Vlachos, *ACS Catal.*, **11**, 8104 (2021).

112. M. Chu, W. Tu, S. Yang, C. Zhang, Q. Li, Q. Zhang and J. Chen, *SusMat*, **2**, 161 (2022).

113. X. Zhang, Y. Lu, L. Kovarik, P. Dasari, D. Nagaki and A. M. Karim, *J. Catal.*, **394**, 376 (2021).

114. B. Coq, R. Dutartre, F. Figueras and T. Tazi, *J. Catal.*, **122**, 438 (1990).

115. J. H. Sinfelt, J. L. Carter and D. J. C. Yates, *J. Catal.*, **24**, 283 (1972).

116. Y. Liu, Q. Zhong, P. Xu, H. Huang, F. Yang, M. Cao, L. He, Q. Zhang and J. Chen, *Matter*, **5**, 1305 (2022).

117. Y. Li, M. Wang, X. Liu, C. Hu, D. Xiao and D. Ma, *Angew. Chem. Int. Ed.*, **61**, e202117205 (2022).

118. I. Vollmer, M. J. F. Jenks, R. Mayorga González, F. Meirer and B. M. Weckhuysen, *Angew. Chem. Int. Ed.*, **60**, 16101 (2021).

119. H. Almohamadi, M. Alamoudi, U. Ahmed, R. Shamsuddin and K. Smith, *Korean J. Chem. Eng.*, **38**, 2208 (2021).

120. J. Lai, Y. Meng, Y. Yan, E. Lester, T. Wu and C. H. Pang, *Korean J. Chem. Eng.*, **38**, 2235 (2021).

Insoo Ro obtained his B.S. degree *magna cum laude* in Chemical Engineering in 2012 from Rice University. He received Ph.D. degree in Chemical Engineering from University of Wisconsin at Madison in 2017 under the supervision of Profs. James Dumesic and George Huber. Following postdoctoral work at University of California at Santa Barbara with Professor Phillip Christopher in the area of single-atom catalysis, Insoo Ro joined Seoul National University of Science and Technology in 2020. He is currently an assistant professor in the Department of Chemical and Biomolecular Engineering. He has published more than 25 papers and has been recognized with several awards including Doh WonSuk Memorial (2016), Kokes Award (2017), Miwon Young Scientist Award (2021), and Young Researcher Award (2021).